Lab on a Chip

Accepted Manuscript

ROYAL SOCIETY OF CHEMISTRY

www.rsc.org/loc

Graphical and textual abstract:

A microfluidic system for the study of T-cell chemotaxis and subsequent gene expression analysis.

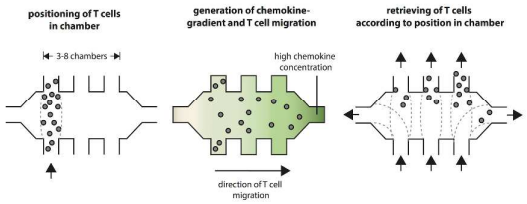

Lab on a Chip

RSCPublishing

ARTICLE

Real-time tracking, retrieval and gene expression analysis of migrating human T cells

Cite this: DOI: 10.1039/xoxxoooooox

Matthias Mehling, Tino Frank, Cem Albayrak, Savaş Tay

Received 3rd September 20124
Accepted

DOI: 10.1039/xoxxoooooox

www.rsc.org/

Dynamical analysis of single-cells allows assessment of the extent and role of cell-to-cell variability, however traditional dish-and-pipette techniques have hindered single-cell analysis in quantitative biology. We developed an automated microfluidic cell culture system that generates stable diffusion-based chemokine gradients, where cells can be placed in predetermined positions, monitored via single-cell time-lapse microscopy, and subsequently be retrieved based on their migration speed and directionality for further off-chip gene expression analysis, constituting a powerful platform for multiparameter quantitative studies of single-cell chemotaxis. Using this system we studied CXCL12-directed migration of individual human primary T cells. Spatiotemporally deterministic retrieval of T cell subsets in relation to their migration speed, and subsequent analysis with microfluidic droplet digital-PCR showed that the expression level of CXCR4 -the receptor of CXCL12- underlies enhanced human T cell chemotaxis.

Introduction

Cell migration has important roles in various physiological processes such as embryogenesis, tissue repair, and especially in immune responses.[1,2] For protective immunity, migration of T cells provides the basis for orchestrated homing and positioning within lymphoid and non-lymphoid tissues.[3] Tissue-specific homing and intra-parenchymal migration of T cells is a highly regulated process at various temporal and spatial scales.[4] Specifically, exposure to chemokine gradients and binding of chemokines to G-protein coupled receptors induces polarization of T cells, and the formation of protrusions where focal adhesions link extracellular matrix proteins to the actin-cytoskeleton result in directed migration towards the gradients.[5] Besides protective immunity, T cell migration is also a key element in the pathogenesis of autoimmune diseases such as multiple sclerosis[6] or Crohn's disease.[7] The majority of the above-described insights in cell migration are based on findings in animal models.

For human T cells, some of the migration-characteristics have been recapitulated in vitro, mostly by the use of transwell assays. Transwell assays such as the Boyden-chamber are robust, allow enumeration of the displacement of individual cells across a membrane and therefore provide a quantitative measure of chemotaxis.[8] However, this approach is unapt to define key aspects impacting the biology of cellular motility in vivo. Specifically, (i) no information can be derived regarding the spatial and temporal stability of chemotactic gradients, (ii) no complex multidirectional gradients of multiple chemoattractants can be established (which will typically be present in an in vivo system), and most importantly (iii) single cells cannot be monitored and characterized in real-time phenotypically or functionally. As a result, most in vitro but also in vivo studies assessed various aspects of T cell migration with a population-averaged manner where migration characteristics at the single cell level were not interrogated.

To characterize migration of human T cells and to aid quantitative studies of chemotaxis, we developed an automated microfluidic cell culture system that significantly surpasses the capabilities of traditional cell culture and migration assays, and characterized migration of primary human CD4+ T cells in gradients of the chemokine CXCL12 using this system. Recently, microfluidic single-cell analysis was used to greatly improve our understanding of immune functions from single cells up to the population level. [9-13] Our system was designed to address limitations of both traditional and existing microfluidic approaches, representing a major advance in single-cell analysis of cell migration. The microfluidic migration device we developed comprises 6 independent cell culture chambers, where in each chamber a diffusion-based

Department of Biosystems Science and Engineering, ETH Zürich, Mattenstrasse 26, 4058 Basel/Switzerland, savas.tay@bsse.ethz.ch
Electronic Supplementary Information (ESI) available: 5 videos, 1 image, 1 supplementary methods file.
See DOI: 10.1039/b000000x/
M. Mehling and T.Frank contributed equally

chemokine gradient can be generated and both adherent and suspension cells can be cultured under flow-free conditions. Our device controls the type, steepness, mean concentration and polarity of each gradient generated in the 6 independent chambers of the device. These gradients are extremely stable with minimal variation of concentration profiles over time, but the gradient type can also be changed when desired without disturbing the cultured cells. By integrating computer control, microfluidic membrane valves and automated microscopy, our system allows precise positioning, monitoring and subsequent retrieval of migrating cells from up to 10 locations inside each nanoliter-sized culture chamber. Real-time quantification of migration via time-lapse microscopy, automated tracking, and subsequent retrieval of cell subpopulations at precisely determined positions allows differential genetic analysis of migrating vs. non-migrating or slow vs. fast cells in the observed population.

Using this system we generated flow-free diffusion-based gradients of the chemokine CXCL12, and tracked primary human CD4+ T cells exposed to these gradients with high spatiotemporal resolution.. Exposure to gradients of CXCL12 induced migration of CD4+ T cells towards higher concentrations in the gradient, increased the migration velocity and track straightness of the cells. Microfludic spatiotemporal retrieval and subsequent droplet digital PCR analysis of the cells in relation to their migration characteristics - i.e. migration towards the gradient or not - revealed that the expression levels of CXCR4 -the receptor of CXCL12- is much greater in cells with enhanced chemotaxis as compared to cells in which no chemotaxis was induced. Taken together we demonstrate here the potential of our microfluidic system to induce primary human T cell migration in diffusion-based chemokine gradients, monitor cell migration of individual cells and retrieve cells with spatiotemporal resolution for off-chip analysis with powerful new gene expression methods like digital-PCR.

Material and Methods

Chip design and fabrication

Transparency photomasks (Fineline Imaging, Colorado Springs, CO, US) were generated using AutoCAD (Autodesk, Inc., San Rafael, CA, US) outline of the designed multi-layer device. Multi-layer PDMS soft-lithography was used for fabrication of chips, as described previously.[14,15] A more detailed description is given in the supplementary methods file.

Chip operation and control

Control channels were connected to solenoid valves (Festo, Dietikon, Switzerland) that were controlled with a custom LabVIEW (National Instruments, Austin, TX, US) graphical user interface and experimental scripts program we wrote, and were electronically controlled using an established control box system.[16] Optimal closing pressures of push-up PDMS membrane valves were individually determined for all used chips, and ranged between 1 – 1.5 bar. A more detailed description is given in the supplementary methods file.

Reagents and surface functionalization

For avoiding undesired attachment of cells flow channels were treated with the copolymer pluronic 10mg/mL (Millipore, Zug , Switzerland) for 3 min, followed by washing with PBS for 30 min. Next, migration chambers were coated with fibronectin at 250mg/mL concentration (Millipore, Zug , Switzerland) for 60 min followed by blocking with RPMI 1640 containing 10% FCS, 50 U/mL penicillin, and 50 mg/mL streptomycin (R10, all from Life Technologies, Zug, Switzerland). R10 containing CXCL12 chemokine at 1μg/mL concentration (Preprotech, London, UK) was used for the generation of chemokine gradients. Cells were harvested for off-chip analysis using 0.05% Trypsin-EDTA (Life Technologies, Zug, Switzerland).

Generation of stable gradients using temporally modulated source–sink flow patterns

Stable diffusion-based chemokine gradients were generated and maintained as previously described by using a switching source-sink flow pattern.[14] Briefly, the channels at the top and the bottom of the cell culture chamber / migration chamber were sequentially refilled with fresh medium either with the chemokine or without it. Therefore a local high concentration (source) and a low concentration was established where as between the gradient is built up and maintained by diffusion. The sink or source was replaced every 4 minutes as reported before.

PBMCs and T-cell isolation

EDTA blood was obtained from healthy volunteers after informed consent (study approved by the institutional review board of both cantons of Basel). PBMCs were isolated from EDTA blood by Ficoll gradient centrifugation using SepMate tubes (Stemcell Technologdies, Grenoble, France). CD4+ T cells were purified by using negative selection with immunomagnetic bead separation (Stemcell Technologies, Grenoble , France). The purity of the isolated CD4+ T-cell population was consistently greater than 95%.

Imaging and data analysis

Cells were tracked using an automated inverted microscope (Nikon Ti, 10x and 20x ELWD Objective) equipped with a stage-top incubator controlling for temperature (37°C), CO_2-concentration (5%) and humidity (90%), a digital CMOS camera (ORCA-Flash 4.0, Hamamatsu Photonics) and the microscope software Nikon AR. Image processing and data analysis was carried out using Imaris with a tracking-tool extension (Bitplane Inc.) and Matlab 2010 (MathWorks Inc.). A more detailed description is given in the supplementary methods file.

Isolation of mRNA, cDNA generation and droplet digital PCR (ddPCR)

Subpopulations of cells harvested from chip were lysed and total RNA was purified from T cells using the RNeasy Mini Kit (Qiagen, Hilden, Germany). Total RNA was used for reverse transcription (Promega, Madison, WI). For droplet digital PCR (ddPCR), 2.6 µl cDNA (final concentration 350 ng/µl) was combined with 10 µl of 2X ddPCR Super Mix for Probes (Bio-Rad), solution primers and probes. Deionized sterile water was added to bring the total volume to 20 µl. The following primers and hydrolysis probe were used: CD3 forward: TCC GAG ATC GAG ATG ATG; CD3 reverse: GGA AGG TAC AGT TGG TAA TG ; CD3 probe: 6FAM- AGG TTC ACT TGT TCC GAG CCC A-BHQ-1. For quantification of CXCR4-expression a CXCR4 TaqMan® Gene Expression Assay (FAM-MGB) was used (LifeTechnologies, Zug, Switzerland). The resultant 20 µl ddPCR solutions were transferred to DG8 cartridges, emulsified by the QX100 Droplet Generator (Bio-Rad); and the emulsions were placed in a Veriti thermal cycler (Life Technologies) for PCR. The temperature schedule for PCR was: 1X, 95°C for 10 min; 40X, 94°C for 30 s followed by 60°C for 1 min; 1X, 98°C for 10 min; and the ramp speed was 2.5°C/s. After, the emulsions were analyzed using the QX100 Droplet Reader and QuantaSoft software (Bio-Rad). Fluorescence from the emulsion droplets was quantified in the Absolute Quantification setting, and the signal threshold was manually set by applying to all wells the threshold value determined by auto-analysis of 1000one of the most concentrated samples.

Statistical analysis

Data nested in the different groups were analyzed with the Kolmogorov-Smirnov test. Mann-Whitney test was performed in the case of non-normality. Data with normal distribution were assessed by paired Student 2-sided t test. Values of $p < 0.05$ were considered to be significant.

Results and Discussion

Microfluidic cell culture system for real-time analysis of single-cell chemotaxis

For assessing cell migration, we developed a microfluidic device that allows (i) localized positioning of human T cells, (ii) the generation of diffusion-based flow-free chemokine gradients in parallel chambers containing cells, (iii) analysis of cell migration with video microscopy and automated tracking and (iv) retrieving of cells according to their position in the chamber, as illustrated in **Figure 1A**. The core component of this 2-layer polydymethylsiloxane (PDMS) device are migration chambers (l= 900µm, w= 250µm, h= 25µm) containing 3-8 ports at both long ends originating from two

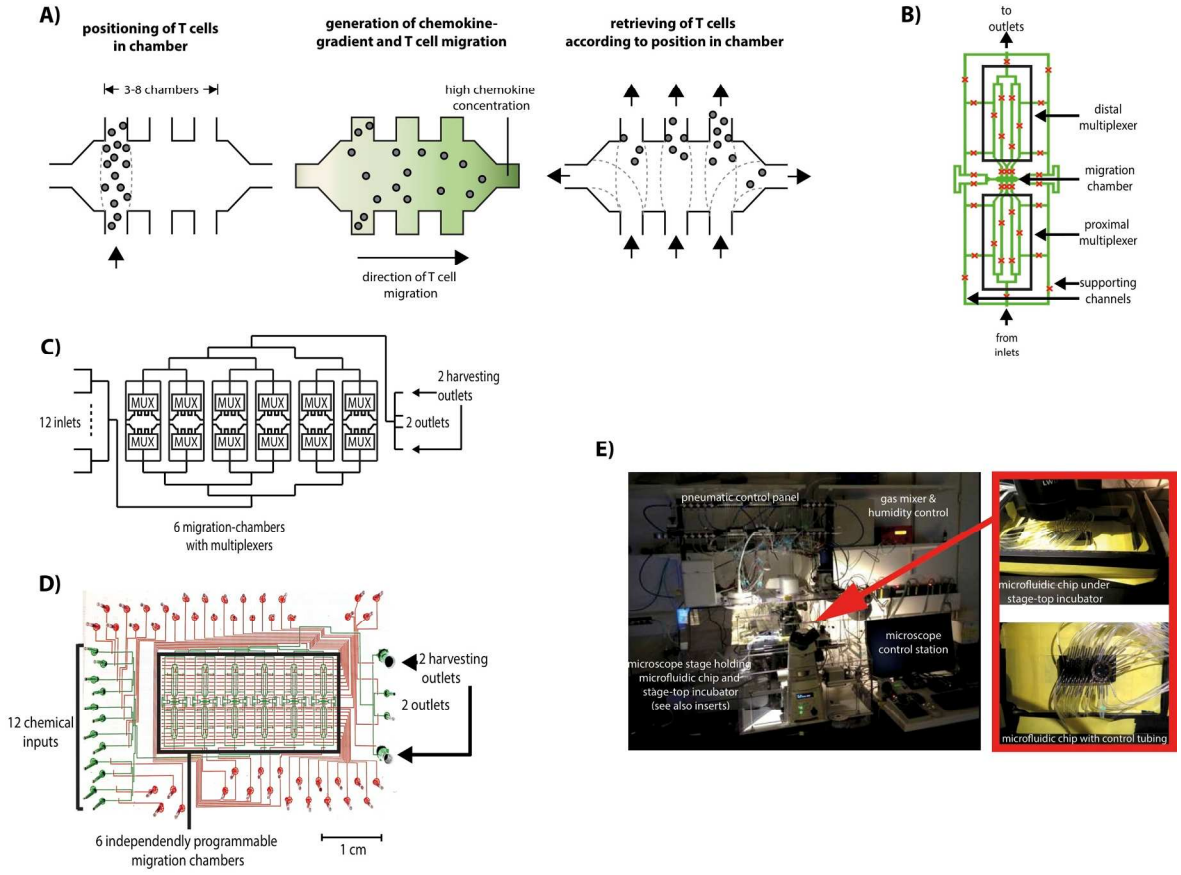

Fig. 1 Overview of microfluidic chemotaxis and cell retrieval device. (A) Schematic overview of the geometry and functionality of an individual microfluidic migration chamber. Cells can be seeded into and be harvested from up to 10 positions inside the gradient chamber using side channels (see SI movie S1). (B) Supplying multiplexer architecture of the 3-side-channel device. (C) Schematic and (D) actual photograph of actual device with 6 microfluidic migration chambers and the respective multiplexers between inlets and outlets (green structures: flow channels; red structures: control channels). (E) Overview of the fully integrated microfluidic system with inserts showing the microfluidic chip mounted on the automated microscope.

multiplexers localized proximally and distally of the **x-position** chamber while the ports at the two short ends of the chamber are connected to support channels (**Figure 1B**). All ports are equipped with independently addressable PDMS membrane valves for controlled flow of fluids and cells. The device contains 6 independent migration chambers, 12 inlets for

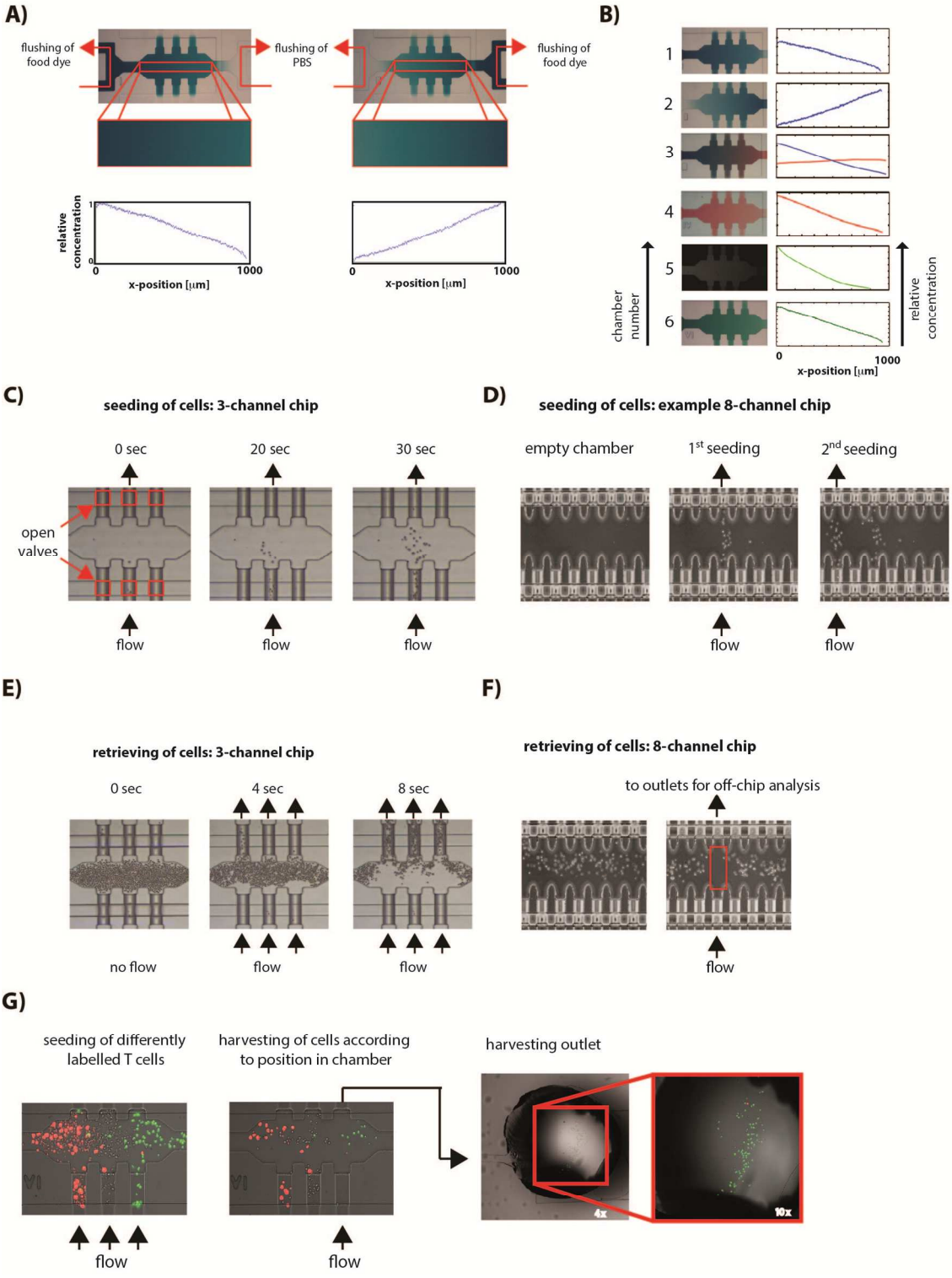

Fig. 2 Functionality of microfluidic chemotaxis and cell retrieval device. (A) Generation of diffusion-based gradients of a dye in microfluidic migration chambers (upper panels) and quantification of the respective relative concentrations in the chambers (lower panels). (B) Example of simultaneous generation of various diffusion-based gradients with food dye (chamber 1-4 and 6) and fluorescent FITC-dextran molecules (chamber 5) with actual pictures of the individual chambers (left column) and measured relative concentrations in the chambers (right column). (C and D) Localized seeding of primary human T cells in microfluidic migration chamber (see also SI movie S2). (E and F) Retrieving of unattached human T cells from microfluidic migration device for off-chip analysis (see SI movie S4). (G) Specific retrieving of attached primary human T cells according to position in the chamber and transfer to harvesting outlet for off-chip analysis. Only green dyed cells can be seen in the harvesting outlet.

reagents and media, and 4 waste and cell harvesting outlets. Support channels connect the reagent inlets with the migration chambers, multiplexers, and the outlets where cells can be retrieved (**Figure 1C**).

The actual assembly of the individual components of the device is given in **Figure 1D,** while **Figure 1E** gives an overview of the full automated microfluidic system. As shown in **Figure 2A/B** and **supplementary movie S1** the device can simultaneously generate 6 independent diffusion-based chemical gradients using a source-sink configuration,[14] and cells can be cultured and monitored in these gradients. By flowing a different molecule (i.e. chemokine) through the source and sink channels that are orthogonal to the migration chamber and allowing diffusion, we can generate flow-free chemokine gradients in the migration chambers where the type, steepness, mean concentration and duration of each gradient can independently be controlled. Spatially and temporally opposing gradients can be generated, and the polarity or ligand type of the gradients can be switched when needed. As the device relies on diffusion for mass transport and not fluid flow, the above-mentioned operations can be performed without disturbing the positions or migration behavior of the cells.[17] The cell culture conditions, including culture media and gas exchange rates and humidity were optimized to allow week-long experiments with excellent cell viability and growth.[18]

To realize a complete system for cell migration studies, we integrated this device to an automated microscope and tracking software, where various tasks including surface treatments, cell seeding, gradient generation and video microscopy is computer controlled through a graphical user interface and custom scripts written in Matlab or
Labview. The combination of automation, nanoliter-sized

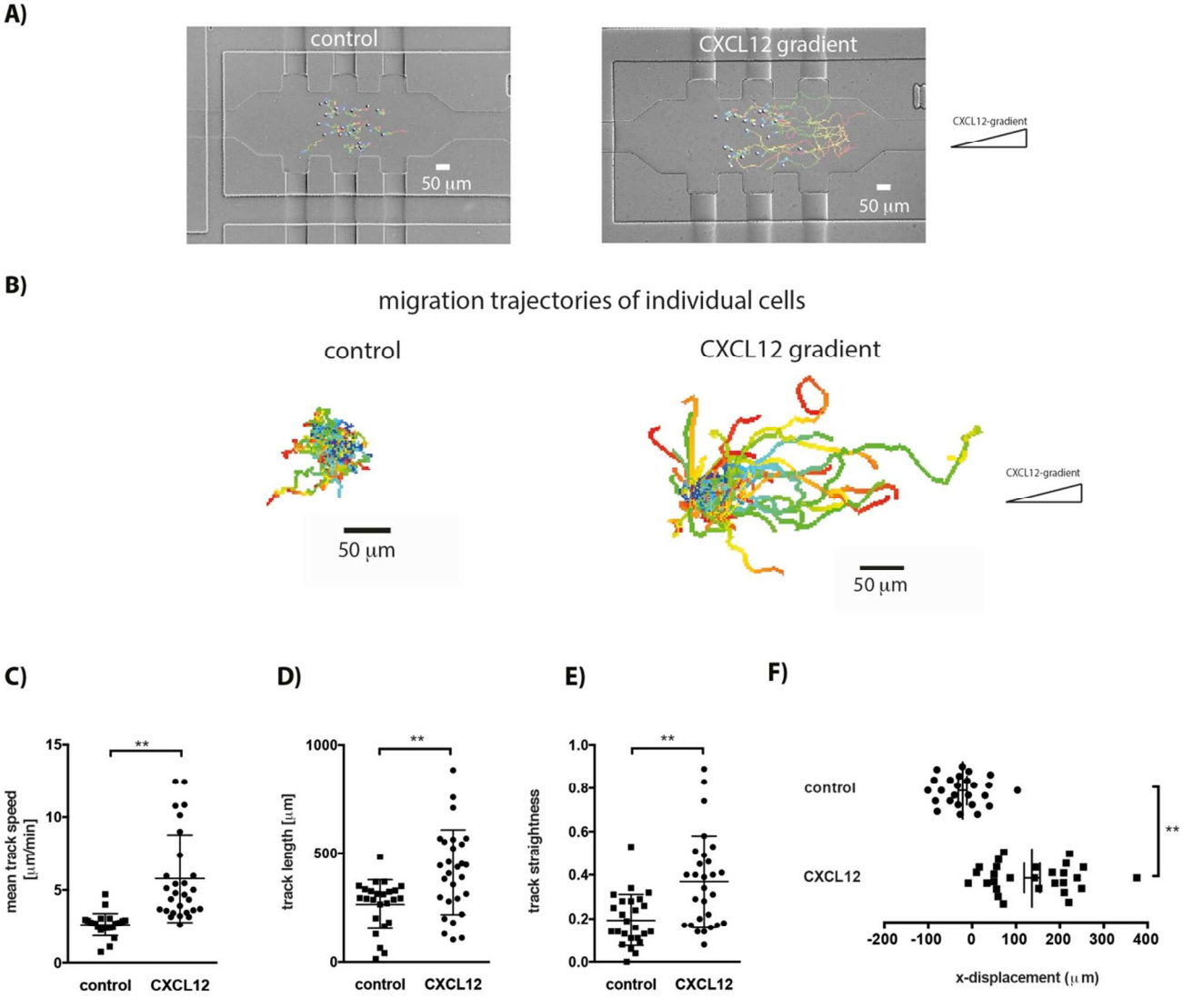

Fig. 3 CXCL12-directed migration of human CD4+ T cells in microfluidic migration device. (A) Overview of microfluidic migration chambers with plotted migration trajectories of CD4+ T cells in the absence (left panel) and the presence of CXCL12 gradient (right panel; color code indicates timepoint during 2h tracking). (B) Trajectories of migrating T cells plotted on a common starting point in the absence (left panel) and presence (right panel) of CXCL12 gradient. (C) Mean migration speed (± SEM, standard error of the mean), (D) mean track length (± SEM) and (E) mean straightness (± SEM) of CD4+ T cells cultured under control conditions or when exposed to the CXCL12-gradient. (F) Mean x-displacement (± SEM) of primary human T cells in the absence (control) or presence of CXCL12 gradient.

chambers and controlled laminar flow conditions allows our system to culture and carefully analyse small populations of cells if needed, constituting a major advantage when working with rare cell types. Use of the multiplexer localized proximally and distally of specific migration chambers allows localized positioning of lymphocytes in distinct sections of the migration chambers. As illustrated in **Figure 2C/D and shown in supplementary movie S2** for primary human CD4+ T cells, lymphocytes can be positioned in specific regions of the migration chamber: for example into an area of 250x200 micrometers in the middle section of the 250x900 micrometer sized culture chamber. Following positioning of the cells, we supply chambers with fresh cell culture medium through diffusion from the sides for 45 minutes to allow attachment of the cells to the ECM-substrate. The cells can be monitored with time-lapse microscopy or stained for immunohistochemistry (**Figure S3**).

When needed the cells can be retrieved from various positions inside the migration chamber using the side-ports and the multiplexer directed towards the cell outlets. **Figure 2E/F** and **supplementary movie S4** illustrate the controlled retrieval of densely seeded T cells from the migration chamber based on their horizontal position. Following retrieval from the migration chamber into the distal multiplexer, cells can be transferred to one of the outlets for retrieval with a pipette and off-chip analysis. If needed, retrieved cells can also be positioned back into the migration chambers without taking them off the chip. For retrieving attached cells from specific regions of the migration chambers, trypsin is gently flown into the migration chamber, and the chamber is then sealed. The cells incubated in trypsin detach from the PDMS substrate within a few minutes, but they remain fixed in their original positions, as there is no convective mixing in the used microfluidic conditions. The detached cells can then be retrieved based on their horizontal positions. To illustrate the specific retrieval of cells, unlabeled cells and cells labeled with calcein red or calcein green were positioned in the middle, the left and the right section of the chamber, respectively (**Figure 2G**). Following attachment, cells were detached and sequentially retrieved from defined regions of the migration chamber by slowly flowing trypsin via the corresponding channels of the multiplexers into harvesting outlets. By doing so, 85 – 90% of labeled cells from specific regions of the migration chamber were harvested sequentially based on their position in the chamber into different harvesting outlets, as shown exemplarily for an outlet that contains calcein green stained cells from the right section of the chamber (**Figure 2G**, right panel). Purity of the retrieved cells in the harvesting outlets ranged between 82% and 90%. Taken together, our system comprises a significant step in analysis of cell migration because it allows precise and if necessary confined positioning of cells in our migration chamber, the establishment and control of diffusion-based chemokine gradients, automated live cell microscopy and cell tracking, and retrieving of individual cells based on their position (i.e. migration speed) in the chamber.

Microfluidic chemotaxis of primary human CD4+ T cells

Migration of human T cells plays a central role in protective immunity but also in the pathogenesis of autoimmune diseases such as MS. The latter is supported by the fact that two highly efficacious drugs for the treatment of MS impact on T cell migration: Fingolimod acts as a functional antagonist on the S1P receptor (S1PR), hereby preventing recirculation of T cells from SLT to peripheral blood;[19] natalizumab blocks adhesion of blood T cells to endothelial cells and as a consequence migration across the blood-brain barrier.[20]

To assess migration characteristics of human T cells, CD4+ T cells were enriched by negative isolation with magnetic beads from healthy donor EDTA-blood and placed in fibronectin-coated microfluidic migration chambers. Following attachment, T cells were either exposed to gradients of CXCL12 by providing CXCL12 containing culture medium from one side of chamber and only medium from other side, or cultured under control conditions by providing cell culture medium from both sides at the same rate. Most T cells cultured under control conditions migrated spontaneously in a non-directional fashion (**Figure 3A/B; and supplementary movie S5**) with a mean track speed (track length [μm] / time [min]) of 2.6 μm/min, resulting in a mean track length of 266 μm during a 2h observation (**Figure 3C/D**). Exposure to a CXCL12 gradient induced migration of T cells (**Figure 3A/B; and supplementary movie S6**) and resulted in significantly increased displacement towards higher concentrations of the gradient (**Figure 3F**). Also, the mean track speed was increased resulting in a significantly longer mean track length of 414 μm (**Figure 3C/D**). Directionality (distance from starting position to final position [μm] / track length [μm]) of cell migration was also significantly increased in cells exposed to a CXCL12 gradient (**Figure 3E**).

Enhanced chemotaxis of CD4+ human T cells in CXCL12 gradients is linked to CXCR4-expression

Migration of human T cells towards chemoattractants has been linked to expression levels of the respective receptors.[21,22] In one study using a transwell migration system, levels of CXCR5-expression in human CD8+ T cells were correlated to chemotactic response towards CCL5, the ligand of CXCR5.[22] Despite the fact that transwell migration systems are unapt to define migration characteristics of lymphocytes on a single cell level, initial sorting of the cells with anti-CXCR5 potentially impacts on migration in gradients with CCL5.

To overcome these limitations we determined levels of CXCR4-expression in primary human T cells following migration experiments in gradients of CXCL12. Specifically, cells were placed at one end of our microfluidic migration device and exposed to a gradient of CXCL12. Following migration of cells in the gradient with video microscopy, we harvested the cells via the side channels of the migration chamber in correlation to their position in the chamber, which corresponds to their chemotactic response to CXCL12. By

doing so we specifically harvested on the one hand a pooled subpopulation of primary human CD4+ T cells that had migrated in gradients of CXCL12 and on the other hand a subpopulation of the same type of cells that had not shown any chemotactic response. We analysed the expression of CXCR4 in both group of pooled cells (~20 cells) using microfluidic droplet-based digital-PCR, which allows absolute copy-number quantitation of nucleic acids.[23,24] Interestingly, we observed significantly higher levels of CXCR4-expression in cells that had migrated strongly in gradients of CXCL12 as compared to cells that had not shown a chemotactic response (**Figure 4A/B**). Taken together these findings indicate that in primary human T cells migration in gradients of CXCL12 is linked to levels of CXCR4-expression.

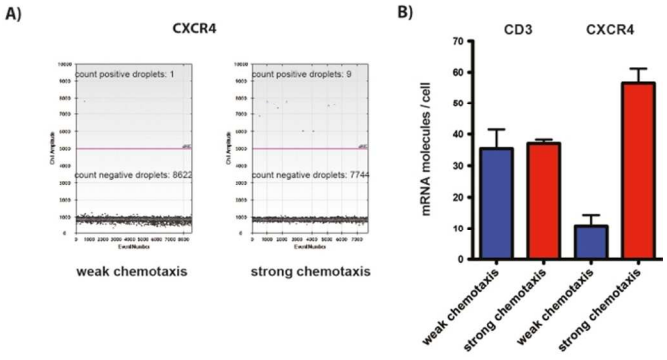

Fig. 4 mRNA expression of chemokine receptor CXR4 in weakly or strongly migrating CD4+ T cells in gradients of the chemokine CXCL12. The cells were harvested from different positions in the migration chamber after chemotaxis, observed under video microscopy. (A) Illustrative plots of digital droplet PCR analysis of CXCR4-mRNA expression. (B) Mean mRNA-expression levels of CD3 (control) and CXCR4 (± SEM; standard error of the mean) in primary human CD4+ T cells in correlation to their migration in gradients of CXCL12 (weak vs. strong chemotaxis).

Conclusion

Migration of primary human T cells is classically studied in vitro by the use of transwell migration assays.[8] These techniques helped recapitulating important insights into T cell migration gained from animal studies also in human T cells. However, transwell migration assays are inherently limited in controllability of experimental conditions, allow assessment of lymphocytes only on a population level, and do not allow real-time longitudinal analysis of individual cells or populations. In this report we addressed these limitations and developed a microfluidic device specifically engineered to study migration of cells, such as primary human T cells. We combined this device with computer control, automated cell tracking and off-chip genetic analysis to realize a complete system and pipeline of protocols for quantitative studies of cell migration. This approach enabled us to (i) generate stable chemokine gradients, (ii) track individual cells in such gradients in real time and (iii) retrieve cells as a function of their position in the device – i.e. their migration characteristics – for further off-chip analysis such as digital gene expression profiling.

Few previous studies addressed T cell migration using non-traditional techniques like microfluidics. One study found increased directed migration towards the chemokine CCL21 compared to CCL19, and no additive effects of these two CCR7-ligands.[25] In contrary, the presence of background CCL21 induced repulsive chemotaxis away from gradients of CCL19, illustrating the significance of studying T cell migration in controllable chemokine gradients. Further, characteristics of T cell migration in competing chemokine gradients of CCL19 and CXCL12 appeared to be related to the specific position of individual cells in the gradients, a finding that would have been masked in bulk assays.[26] These highlighted the importance of studying T cell migration under controlled conditions with high spatio-temporal resolution and on a single cell level. However, these studies are based on microfluidic devices in which the gradients are generated using parallel streams of laminar flow across the culture chamber, hereby significantly contrasting the flow-free nature of in-vivo chemokine-gradients. Further, spatially specific retrieval of migrating cells or different subpopulations based on migration speeds has not been possible from microfluidic devices before this study.

As a proof of concept of these functionalities, we assessed expression levels of the CXCL12-receptor CXCR4 in primary human CD4+ T cells as function of their migration towards higher concentrations of CXCL12. Cells responding to CXCL12 expressed significantly higher levels of CXCR4 mRNA as compared to cells that did not migrate in gradients of CXCL12. These observations are in line with a previous study that linked expression levels of CXCR5 on T cells with migratory responses towards the CXCR5-ligand CCL5.[22] In this study CD4+ and CD8+ T cells were sorted and subjected to CCL5-directed migration exclusively on the basis of CXCR5-expression, which was not assessed in T cell subpopulations. Taken together, our microfluidic migration device allows linking expression levels of given molecules as a function of migration characteristics of specific individual cells, which has the potential to significantly add to our understanding of how migration of cells is regulated on a single cell level.

Acknowledgements

M.M. is supported by the University of Basel Research Grant, the Swiss Multiple Sclerosis Society and the Novartis Foundation. S. T. acknowledges support from the ERC Starting Grant 337986 (SingleCellDynamics), Swiss National Science Foundation, SNF Systems X Grant NeuroStemX and Swiss NCCR Molecular Systems Engineering. We thank Th. Horn and A. Ponti from the Single Cell Facility of the DBSSE of the ETH Zürich for support with imaging and image analysis.

References

1. Lämmermann, T. & Sixt, M. The microanatomy of T-cell responses. *Immunol. Rev.* **221,** 26–43 (2008).
2. Horwitz, R. & Webb, D. Cell migration. *Curr. Biol.* **13,** R756–9 (2003).
3. Andrian, von, U. H. & Mempel, T. R. Homing and cellular traffic in lymph nodes. *Nature Reviews Immunology* **3,** 867–878 (2003).
4. Friedl, P. & Weigelin, B. Interstitial leukocyte migration and immune function. *Nat Immunol* **9,** 960–969 (2008).
5. Swaney, K. F., Huang, C.-H. & Devreotes, P. N. Eukaryotic Chemotaxis: A Network of Signaling Pathways Controls Motility, Directional Sensing, and Polarity. *Annu. Rev. Biophys.* **39,** 265–289 (2010).
6. Sallusto, F. *et al.* T-cell trafficking in the central nervous system. *Immunol. Rev.* **248,** 216–227 (2012).
7. Marsal, J. & Agace, W. W. Targeting T-cell migration in inflammatory bowel disease. *J. Intern. Med.* **272,** 411–429 (2012).
8. Falasca, M., Raimondi, C. & Maffucci, T. Boyden chamber. *Methods Mol. Biol.* **769,** 87–95 (2011).
9. Vedel, S., Tay, S., Johnston, D. M., Bruus, H. & Quake, S. R. Migration of cells in a social context. *Proc. Natl. Acad. Sci. U.S.A.* **110,** 129–134 (2013).
10. Kam, L. C., Shen, K. & Dustin, M. L. Micro- and Nanoscale Engineering of Cell Signaling. *Annu Rev Biomed Eng* **15,** 305–326 (2013).
11. Melin, J. & Quake, S. R. Microfluidic Large-Scale Integration: The Evolution of Design Rules for Biological Automation. *Annu. Rev. Biophys. Biomol. Struct.* **36,** 213–231 (2007).
12. Tay, S. *et al.* Single-cell NF-κB dynamics reveal digital activation and analogue information processing. *Nature* **466,** 267–271 (2010).
13. Mazutis, L. *et al.* Single-cell analysis and sorting using droplet-based microfluidics. *Nat Protoc* **8,** 870–891 (2013).
14. Frank, T. & Tay, S. Flow-switching allows independently programmable, extremely stable, high-throughput diffusion-based gradients. *Lab Chip* **13,** 1273–1281 (2013).
15. Unger, M. A., Chou, H. P., Thorsen, T., Scherer, A. & Quake, S. R. Monolithic microfabricated valves and pumps by multilayer soft lithography. *Science* **288,** 113–116 (2000).
16. Gómez-Sjöberg, R., Leyrat, A. A., Pirone, D. M., Chen, C. S. & Quake, S. R. Versatile, fully automated, microfluidic cell culture system. *Anal. Chem.* **79,** 8557–8563 (2007).
17. Walker, G. M. *et al.* Effects of flow and diffusion on chemotaxis studies in a microfabricated gradient generator. *Lab Chip* **5,** 611–618 (2005).
18. Kellogg, R. A., Gómez-Sjöberg, R., Leyrat, A. A. & Tay, S. High-throughput microfluidic single-cell analysis pipeline for studies of signaling dynamics. *Nat Protoc* **9,** 1713–1726 (2014).
19. Mehling, M., Johnson, T. A., Antel, J., Kappos, L. & Bar-Or, A. Clinical immunology of the sphingosine 1-phosphate receptor modulator fingolimod (FTY720) in multiple sclerosis. *Neurology* **76,** S20–7 (2011).
20. Derfuss, T., Kuhle, J., Lindberg, R. & Kappos, L. Natalizumab Therapy for Multiple Sclerosis. *Semin Neurol* **33,** 026–036 (2013).
21. Qin, S. *et al.* Expression of monocyte chemoattractant protein□1 and interleukin□8 receptors on subsets of T cells: correlation with transendothelial chemotactic potential. *Eur J Immunol* **26,** 640–647 (1996).
22. Desmetz, C. *et al.* The strength of the chemotactic response to a CCR5 binding chemokine is determined by the level of cell surface CCR5 density. *Immunology* **119,** 551–561 (2006).
23. Tawfik, D. S. & Griffiths, A. D. Man-made cell-like compartments for molecular evolution. *Nat Biotechnol* **16,** 652–656 (1998).
24. Dressman, D., Yan, H., Traverso, G., Kinzler, K. W. & Vogelstein, B. Transforming single DNA molecules into fluorescent magnetic particles for detection and enumeration of genetic variations. *Proc. Natl. Acad. Sci. U.S.A.* **100,** 8817–8822 (2003).
25. Nandagopal, S., Wu, D. & Lin, F. Combinatorial Guidance by CCR7 Ligands for T Lymphocytes Migration in Co-Existing Chemokine Fields. *PLoS ONE* **6,** e18183 (2011).
26. Lin, F. & Butcher, E. C. T cell chemotaxis in a simple microfluidic device. *Lab Chip* **6,** 1462–1469 (2006).

